Scientific Research Publishing

Applied Mathematics, 2021, 12, 1189-1209
https://www.scirp.org/journal/am
ISSN Online: 2152-7393
ISSN Print: 2152-7385

A Comprehensive Price Prediction System Based on Inverse Multiquadrics Radial Basis Function for Portfolio Selection

Mengmeng Zheng

Jinan University, Guangzhou, China
Email: mengmeng@stu2019.jnu.edu.cn

How to cite this paper: Zheng, M.M. (2021) A Comprehensive Price Prediction System Based on Inverse Multiquadrics Radial Basis Function for Portfolio Selection. *Applied Mathematics*, **12**, 1189-1209.
https://doi.org/10.4236/am.2021.1212076

Received: November 14, 2021
Accepted: December 19, 2021
Published: December 22, 2021

Abstract

Price prediction plays a crucial role in portfolio selection (PS). However, most price prediction strategies only make a single prediction and do not have efficient mechanisms to make a comprehensive price prediction. Here, we propose a comprehensive price prediction (CPP) system based on inverse multiquadrics (IMQ) radial basis function. First, the novel radial basis function (RBF) system based on IMQ function rather than traditional Gaussian (GA) function is proposed and centers on multiple price prediction strategies, aiming at improving the efficiency and robustness of price prediction. Under the novel RBF system, we then create a portfolio update strategy based on kernel and trace operator. To assess the system performance, extensive experiments are performed based on 4 data sets from different real-world financial markets. Interestingly, the experimental results reveal that the novel RBF system effectively realizes the integration of different strategies and CPP system outperforms other systems in investing performance and risk control, even considering a certain degree of transaction costs. Besides, CPP can calculate quickly, making it applicable for large-scale and time-limited financial market.

Keywords

Comprehensive Price Prediction, Portfolio Selection (PS), Inverse Multiquadrics (IMQ) Radial Basis Function

1. Introduction

The target of PS is to achieve some long-term financial goals by constructing an effective investment strategy that can reasonably allocate wealth among a set of assets. There are two main theories about PS. One is the mean-variance theory

[1], which aims to balancing the expected return (mean) and risk (variance) of a portfolio and is generally applicable to the single-period PS. The other is Kelly investment [2] [3] which focuses on maximizing the expected log return and is suitable for multiple-period PS. These two theories are also the cornerstone of modern PS research and are constantly exploited and innovated. Considering the real financial market environment, most portfolio researches are more in line with the Kelly investment model. In other words, the essence of PS can be understood as an optimization problem on expected log return. Therefore, in order to make portfolio selection more effective under known historical price information, price prediction is an important link to the construction of portfolio.

Adam's theory mentioned that there was a high chance that the market would go towards a particular direction [4]. Therefore, price prediction plays an indispensable role in PS. At present, the most commonly used price prediction systems generally follow three principles, namely, trend-following principle, trend-reversing principle and pattern-matching principle [5]. Trend-following principle assumes that a well-performing asset's price will keep rising over next period, and vice versa. For example, PPT [6] exploits the maximum value of asset prices within a time window to predict future prices. In contrast to the trend-following, the trend-reversing principle assumes that future asset prices will reverse to some kinds of historical mean. The investment behavior is to sell good performance and buy poor performance [7] [8] [9] [10]. For example, RMR and OLMAR exploit L_1-median [8] and the exponential moving average (EMA) [10], respectively, to make future price prediction. Pattern-matching principle is to look for historical price pattern that fit the current financial environment and use it to predict the future prices [11] [12] [13].

Although some strategies mentioned above can be applied to some data sets with encouraging results, no attempt has been made to combine these strategies to construct a comprehensive price prediction system. In fact, the exponential moving average (EMA) [5], the PP [6] and L_1-median [8] are all classic and widely used price prediction tools. L_1-median and EMA are both moderate strategies, while PP is an aggressive strategy that can actively strive for high returns. Depending on the financial environment, sometimes aggressive strategies are needed to achieve high returns, while sometimes moderate strategies are needed to avoid risks. This inspires us to construct a system able to take full advantage of multiple strategies.

Radial basis functions (RBF) are widely exploited in solving partial differential equations and image denoising, [14]-[21]. The Gaussian (GA) function, the multiquadrics (MQ) function and inverse multiquadrics (IMQ) function are three classic expressions of RBF [20] [22]. Despite its good smoothing effect, GA is a function only with good local characteristics, which means it's significant merely in a neighborhood near the center point. MQ was originally introduced by Hardy [23] and generally accepted by researchers. Although Franke [24]

proved that MQ performed best in dealing with the interpolation problem of scatter data, MQ was conditionally positive definite. Therefore, a more application-oriented IMQ was proposed. The outstanding advantages of IMQ are good global feature, strict positive definite and stable eigenvalue [14] [18]. For example, Abbasbandy [14] pointed out that IMQ could be used to approximate the unknown analytic function to get a more stable and accurate solution in solving the global optimization problem. And Tanbay [19] pointed out that compared with GA in the solution of the neutron diffusion equation, IMQ had a more stable performance and could obtain highly numerical solution. Therefore, we incorporate IMQ rather than traditional GA in our novel RBF system to increase efficiency and robustness.

In this paper, a comprehensive price prediction (CPP) system based on IMQ radial basis function is constructed. The system firstly uses IMQ basis function to construct a novel RBF system. Then, combining with the novel RBF system, a portfolio update strategy based on kernel and trace operator is constructed. Now let's consider H different price prediction strategies. This paper mainly focuses on three strategies, namely EMA, L_1-median and PP. Firstly, CPP selects the best-performing strategy according to investing performance of all strategies within the recent window and given it the largest influence in future price prediction. Secondly, CPP exploits the similarity between the best-performing strategy and other price prediction strategies to calculate the influence of other strategies. This system effectively integrates the advantages of all price prediction strategies and innovative measuring the influence by investing performance. In genneral, this paper's main contributions are as follows:

1) Propose a novel RBF system based on IMQ radial basis function and centered on multiple price predictions, which form a comprehensive price prediction.

2) Propose a comprehensive combination of aggressive strategies and moderate strategies to achieve a better balance between returns and risks.

3) Propose a portfolio update strategy based on kernel and trace operator.

The rest parts of this paper are presented as follows. Section 2 describes the relevant problem setting and related work about PS. The CPP system is introduced and described in detail in Section 3. Experiments on 4 benchmark data sets are carried out to assess CPP in Section 4. Finally, conclusions are presented in Section 5.

2. The Relevant Problem Setting and Related Work

2.1. The Relevant Problem Setting

In this paper, d assets with a time span of n periods in financial market are considered. For the sake of understanding, let's think of a period as a day. The asset prices of the tth period is presented by the close prices vector $\boldsymbol{q}_t \in \mathbb{R}_+^d$, $t = 0,1,2,\cdots,n$, where q_t^i represents the price of the ith asset and $\mathbb{R}_+^d$ is a d-dimensional nonnegative real space. The change of asset prices is presented by

the price relative vector [25]

$$\boldsymbol{s}_t = \frac{\boldsymbol{q}_t}{\boldsymbol{q}_{t-1}}, \quad \boldsymbol{s}_t \in \mathbb{R}_+^d, \quad t = 1, 2, 3, \cdots, n, \tag{1}$$

where division between two vectors represents the division of corresponding components, *i.e.* $s_t^i = \frac{q_t^i}{q_{t-1}^i}$. Note that the price relative vector is an crucial metric in PS, because it's always used to evaluate the performance of an asset. When $\boldsymbol{s}_t^i > 1$, the ith asset price goes up, and vice versa. Of course when $\boldsymbol{s}_t^i = 1$, it means the price doesn't change.

At the beginning of each trading period, wealth needs to be allocated across a range of assets. In this paper, when investing, the proportion of each asset in total weath is recorded as the portfolio vector. Suppose there are d assets and their portfolio vector in the tth period is

$$\boldsymbol{v}_t \in \Delta_d := \left\{ \boldsymbol{v} \in \mathbb{R}_+^d : \sum_{i=1}^{d} \boldsymbol{v}^{(i)} = 1 \right\}, \tag{2}$$

where Δ_d is a d-dimensional simplex. A non-negative constraint indicates that non-short-selling and the equality constraint indicates that self-financing, which means it is not allowed to borrow money and all of the wealth is reinvested. Since all the wealth in the previous periods is invested over next period, the cumulative wealth (CW) increases at a multiple rate, *i.e.* $W_t = W_{t-1}\boldsymbol{v}_t^{\mathrm{T}}\boldsymbol{s}_t$, which $\boldsymbol{v}_t^{\mathrm{T}}\boldsymbol{s}_t$ is the increasing factor. So after n periods, the final cumulative wealth is

$$W_n = W_0 \prod_{t=1}^{n} \left(\boldsymbol{v}_t^{\mathrm{T}} \boldsymbol{s}_t \right), \tag{3}$$

where W_0 is the initial wealth. In this paper, for the convenience of calculation, it is assumed that $W_0 = 1$. Then the final cumulative wealth W_n is

$$W_n = \prod_{t=1}^{n} \left(\boldsymbol{v}_t^{\mathrm{T}} \boldsymbol{s}_t \right). \tag{4}$$

The ultimate purpose of PS system is to maximize the final cumulative wealth W_n by constructing a set of the portfolio vectors $\{\boldsymbol{v}_t\}_{t=1}^n$, that is

$$\tilde{W}_n = \max_{\{\boldsymbol{v}_t \in \Delta_d\}_{t=1}^n} \prod_{t=1}^{n} \left(\boldsymbol{v}_t^{\mathrm{T}} \boldsymbol{s}_t \right). \tag{5}$$

From the above equation, this is equivalent to maximizing the increasing factor $\boldsymbol{v}_t^{\mathrm{T}}\boldsymbol{s}_t$. Note that this optimization problem does not require statistical assumption about the changes in asset price.

2.2. Related Work

In this subsection, some classical prediction strategies are introduced to help us understand how to build a PS system.

The UBAH strategy [5], which is generally used as a market strategy to generate a market index, is to start with an equal distribution of wealth among d assets and keep it constant, thus the final cumulative wealth

$$W_n^{Market} = \frac{1}{d}\sum_{i=1}^{d}\prod_{t=1}^{n} \boldsymbol{s}_t^{(i)}. \tag{6}$$

Both OLMAR [10] and RMR [8], which keep a moderate attitude, use the mean reversion phenomenon to predict the future asset prices. OLMAR points out that the future asset prices would recover to historical moving average and proposed the exponential moving averages (EMA). The EMA exploits all historical price information to achieve price prediction. The specific representation of EMA is as follow:

$$\begin{aligned}\tilde{\boldsymbol{s}}_{E,t+1}(\alpha) &= \frac{EMA_t(\alpha)}{\boldsymbol{q}_t} = \frac{\alpha\boldsymbol{q}_t + (1-\alpha)EMA_{t-1}(\alpha)}{\boldsymbol{q}_t} \\ &= \alpha\mathbf{1} + (1-\alpha)\frac{EMA_{t-1}}{\boldsymbol{q}_{t-1}}\frac{\boldsymbol{q}_{t-1}}{\boldsymbol{q}_t} \\ &= \alpha\mathbf{1} + (1-\alpha)\frac{\tilde{\boldsymbol{s}}_{E,t}}{\boldsymbol{s}_t},\end{aligned} \tag{7}$$

where EMA_t represents the previous EMA and $\mathbf{1}$ is a d-dimensional vector with components of 1. $0 < \alpha < 1$ is a decaying factor and $\boldsymbol{s}_t$ is the real price relative on the tth period.

When expanding EMA_t, then

$$\begin{aligned}EMA_t &= \alpha\boldsymbol{q}_t + (1-\alpha)EMA_{t-1} \\ &= \alpha\boldsymbol{q}_t + (1-\alpha)\alpha\boldsymbol{q}_{t-1} + (1-\alpha)^2 EMA_{t-2} \\ &= \sum_{k=0}^{t-1}(1-\alpha)^k \alpha\boldsymbol{q}_{t-k} + (1-\alpha)^t \boldsymbol{q}_0,\end{aligned} \tag{8}$$

as a result, EMA really makes full use of all historical prices and gives lager weight to more recent price information.

Unlike OLMAR, RMR no longer uses the simple mean, but instead exploits the robustness of L_1-median [26] [27] to predict the future asset prices. Statistically speaking, the L_1-median has a more attractive property than the simple mean because it's breakdown point is 0.5, meaning that when 50% of the points in the data set are pollution values, the L_1-median can take values that exceed all boundaries. A higher the breakdown point means a more stable estimator, and the breakdown point of the simple mean is 0. The corresponding future price relative of RMR is

$$\tilde{\boldsymbol{s}}_{L,t+1} = \frac{L_1 med_{t+1}(\omega)}{\boldsymbol{q}_t}, \tag{9}$$

where

$$L_1 med_{t+1}(\omega) = \arg\min_{\mu} \sum_{i=0}^{k-1} \left\| \boldsymbol{q}_{t-i} - \mu \right\|, \tag{10}$$

where $\|\cdot\|$ represents the Euclidean norm.

OLMAR and RMR exploit the same optimization approach to update strategies as follows:

$$\hat{\boldsymbol{v}}_{t+1} = \arg\min_{\boldsymbol{v}\in\Delta_d} \frac{1}{2}\left\| \boldsymbol{v} - \hat{\boldsymbol{v}}_t \right\|^2, \text{ s.t } \boldsymbol{v}^{\mathrm{T}}\boldsymbol{s}_{t+1} \geq \varepsilon > 0. \tag{11}$$

EMA and L_1-median essentially exploits the principle of mean reversion. They are cautious in their price prediction. However, there are plenty of evidence in real financial markets that irrational investment can keep prices trends. Therefore, the importance of trend-following strategies should not be ignored. In real financial markets, most investors profit from rising prices. So they are more concerned about recent maximum prices. PPT system suggests using the PPs from different asset prices within a time window [6].

$$\tilde{\boldsymbol{q}}_{t+1}^{i} = \max_{0\le k\le \omega-1} \boldsymbol{q}_{t-k}^{i},\ i=1,2,\cdots,d$$

$$\tilde{\boldsymbol{s}}_{P,t+1} = \frac{\tilde{\boldsymbol{q}}_{t+1}}{\boldsymbol{q}_t}, \tag{12}$$

and $\tilde{\boldsymbol{s}}_{P,t+1}$ can also be understood as the growth potential of the assets.

EMA and L_1-median belong to the trend-reversing, both of which are conservative and moderate investment strategies. In contrast, PP is an active and aggressive strategy as it belongs to the trend-following. Depending on the financial environment, sometimes aggressive strategies are needed to achieve high returns, while sometimes moderate strategies are needed to avoid risks. All of these motivate us to construct a comprehensive price prediction system that can effectively integrate the advantages of different strategies.

3. A Comprehensive Price Prediction Based on Inverse Multiquadrics Radial Basis Function

3.1. Novel RBF System Based on IMQ Function

The classical expression of RBF system is as follow:

$$\begin{aligned} &\boldsymbol{y} = \boldsymbol{Q}\boldsymbol{\psi}(\boldsymbol{x}), \boldsymbol{\psi} = [\psi_1, \psi_2, \cdots, \psi_H]^{\mathrm{T}} \\ &\psi_h(\boldsymbol{x}) = \exp\left(\frac{-\|\boldsymbol{x}-\boldsymbol{\rho}_h\|^2}{2\sigma_h^2}\right) \end{aligned} \tag{13}$$

where $\boldsymbol{x}$ and $\boldsymbol{y}$ are input and output respectively, $\boldsymbol{Q} \in \mathbb{R}^{d\times H}$ represents the weight matrix of the RBF system, d is the dimension of output, $\boldsymbol{\psi}$ is a vector composed of GA radial basis function, both $\boldsymbol{\rho}_h$ and σ_h^2 are the center points and the scale parameters of the GA function, respectively. Note that σ_h^2 reflects the width of the function image.

Besides GA, IMQ is another radial basis function that cannot be ignored. Here, a novel RBF system based on IMQ radial basis function is constructed, that is

$$\begin{aligned} &\boldsymbol{y} = \boldsymbol{Q}\boldsymbol{\psi}(\boldsymbol{x}), \boldsymbol{\psi} = [\psi_1, \psi_2, \cdots, \psi_H]^{\mathrm{T}} \\ &\psi_h(\boldsymbol{x}) = \frac{1}{\sqrt{\|\boldsymbol{x}-\boldsymbol{\rho}_h\|^2 + \sigma_h^2}} \end{aligned} \tag{14}$$

There is a theoretical basis for this improvement. GA and IMQ are essentially the same and both are positive definite functions [28]. However, in practical application, IMQ performance is more stable and better than GA [14] [19].

As for the formula in this paper, H price prediction strategies are denoted as

$\left\{\tilde{\boldsymbol{s}}_{h,t+1}\right\}_{h=1}^{H}$. In this paper, three typical price prediction strategies are integrated, namely $\tilde{\boldsymbol{s}}_{E,t+1}$, $\tilde{\boldsymbol{s}}_{L,t+1}$ and $\tilde{\boldsymbol{s}}_{P,t+1}$ in formula Equation (7), Equation (9) and Equation (12), corresponding to $H=3$. The next step is to determine the input $\boldsymbol{x}$ and the center $\boldsymbol{\rho}_h$. First, all price prediction strategies $\left\{\tilde{\boldsymbol{s}}_{h,t+1}\right\}_{h=1}^{3}$ serve as the centers of novel RBF system. Secondly, projection operation is exploited to get qualified portfolio $\tilde{\boldsymbol{v}}_{h,t+1}$, and then choose the strategy with the best performance as the input. The specific methods are as follows:

$$\tilde{\boldsymbol{v}}_{h,t+1}=\arg\min_{\boldsymbol{s}\in\Delta_d}\left\|\boldsymbol{s}-\tilde{\boldsymbol{s}}_{h,t+1}\right\|^2,\ h=1,2,3 \tag{15}$$

$$\tilde{\boldsymbol{s}}_{*,t+1}=\arg\min_{1\le h\le 3}\min_{0\le k\le \omega-1}\tilde{\boldsymbol{v}}_{h,t-k}^{\mathrm{T}}\boldsymbol{s}_{t-k}, \tag{16}$$

where Δ_d is defined as Equation (2) in Equation (15), $\tilde{\boldsymbol{v}}_{h,t-k}^{\mathrm{T}}\boldsymbol{s}_{t-k}$ represents the increasing factor of the *h*th price prediction strategy of the $(t-k)$ th period and $\boldsymbol{s}_{t-k}$ is the actual price relative generated by Equation (1). The method is firstly transformed $\left\{\tilde{\boldsymbol{s}}_{1,t+1},\tilde{\boldsymbol{s}}_{2,t+1},\tilde{\boldsymbol{s}}_{3,t+1}\right\}$ onto a *d*-dimensional simplex [31]. Then it exploits $\left\{\tilde{\boldsymbol{v}}_{h,t-k}\right\}_{k=0}^{w-1}$ generate the increasing factors to evaluate the investing performance and select the input $\tilde{\boldsymbol{s}}_{*,t+1}$ of the novel system. The essence of $\tilde{\boldsymbol{s}}_{*,t+1}$ is select the best-performing strategy, where the best-performing strategy means that it can get the highest return even in the worst financial environment. The general process is that the smallest increasing factors of each strategy is selected within a time window, and then the largest increasing factor is selected from a set composed of the smallest increasing factors. This approach ensures that we get the best price prediction strategy in the worst trading environment, which is the key to improving the overall robustness of the system.

In the novel RBF system mentioned in Equation (14), all qualified portfolios calculated by Equation (15) serve as centers of the novel RBF system, and the best strategy $\tilde{\boldsymbol{s}}_{*,t+1}$ serves as fixed inputs. The specific form of novel RBFs in Equation (14) is transformed into

$$\begin{aligned}&\Delta\boldsymbol{v}_{t+1}=\tilde{\boldsymbol{S}}_{t+1}\boldsymbol{\psi}\left(\tilde{\boldsymbol{s}}_{*,t+1}\right),\boldsymbol{\psi}=\left[\psi_1,\psi_2,\psi_3\right]^{\mathrm{T}}\\&\psi_h\left(\tilde{\boldsymbol{s}}_{*,t+1}\right)=\frac{1}{\sqrt{\left\|\tilde{\boldsymbol{s}}_{*,t+1}-\tilde{\boldsymbol{v}}_{h,t+1}\right\|^2+\sigma_h^2}},\ h=1,2,3\end{aligned} \tag{17}$$

where $\Delta\boldsymbol{v}_{t+1}$ represents the updated increment of the portfolio on the $(t+1)$ th period and $\tilde{\boldsymbol{S}}_{t+1}=\left[\tilde{\boldsymbol{s}}_{1,t+1},\tilde{\boldsymbol{s}}_{2,t+1},\tilde{\boldsymbol{s}}_{3,t+1}\right]\in\mathbb{R}^{d\times 3}$ is equivalent to the weight matrix. The reason for this representation of $\Delta\boldsymbol{v}_{t+1}$ will be explained in the later Section 3.3. From the above formula, it can be seen that the system quantifies the similarity degree between $\tilde{\boldsymbol{s}}_{*,t+1}$ and $\tilde{\boldsymbol{v}}_{h,t+1}$. If $\tilde{\boldsymbol{v}}_{h,t+1}$ is close to $\tilde{\boldsymbol{s}}_{*,t+1}$, then the function ψ_h will increase, and $\tilde{\boldsymbol{s}}_{h,t+1}$ will amplify its influence on the increment $\Delta\boldsymbol{v}_{t+1}$. With the change of the time *t*, the input $\tilde{\boldsymbol{s}}_{*,t+1}$ also changes between different strategies in order to adapt to the latest changes in the financial environment.

The proposed novel RBF system in Equation (17) is different from in Equation (13) in many different ways which are mainly reflected in the problem set-

ting, data characteristics and the selection of radial basis functions.

1) The centers $\{\rho_h\}$ in Equation (13) are obtained by minimizing the error of fitting y. While the centers $\{\tilde{v}_{h,t+1}\}$ in Equation (17) represent the corresponding price prediction strategies.

2) Although the inputs of those two RBF systems are fixed, $\tilde{s}_{*,t+1}$ is determined by the recent investing performance of all prediction strategies. This means that each price prediction strategy is likely to be an input.

3) The basis functions of those two RBF systems are different. The system in Equation (13) uses Gaussian radial basis function, while Equation (17) uses the IMQ radial basis function.

4) The objective of Equation (13) is to fit y. So the back-propagation methods can be used to solve the problem [29] [30]. However, the objective of Equation (17) aims to maximize the generalized increasing factor and the solution method is different from Equation (13).

3.2. Comprehensive Price Prediction System

In order to apply the theory to practice, the next step is to construct a PS model using the proposed novel RBF system. As described in Section 2.1, in order to obtain better investing performance, the increasing factor $\boldsymbol{v}_{t+1}^{\mathrm{T}}\boldsymbol{s}_{t+1}$ should be maximized when price information of t periods is known. Although the price relative $\boldsymbol{s}_{t+1}$ is unknown, we can use the price prediction strategy $\{\tilde{\boldsymbol{s}}_{h,t+1}\}$ to generate the future price relative. In addition, the novel RBF system can be exploited to construct a generalized increasing factor as follow:

$$\begin{aligned} &\boldsymbol{v}_{t+1} = \arg\max_{\boldsymbol{v}} tr\left(\boldsymbol{V}\boldsymbol{\Psi}\tilde{\boldsymbol{S}}_{t+1}^{\mathrm{T}}\right), \boldsymbol{V} = \boldsymbol{v}\boldsymbol{1}_{(3)}^{\mathrm{T}} \\ &\boldsymbol{\Psi} = diag\left(\boldsymbol{\psi}\right), \tilde{\boldsymbol{S}}_{t+1} = \left[\tilde{\boldsymbol{s}}_{1,t+1}, \tilde{\boldsymbol{s}}_{2,t+1}, \tilde{\boldsymbol{s}}_{3,t+1}\right] \\ &\text{s.t. } \boldsymbol{v} \in \Delta_d, \left\|\boldsymbol{v} - \hat{\boldsymbol{v}}_t\right\| \le \varepsilon, \varepsilon > 0, \end{aligned} \tag{18}$$

where tr is the trace operator, $\boldsymbol{V}$ is an 3-dimensional vector with component $\boldsymbol{v}$, $\boldsymbol{\Psi}$ is a diagonal matrix with $\boldsymbol{\psi}$ as diagonal elements, $\tilde{\boldsymbol{S}}_{t+1}$ is a matrix composed of 3 predicted future price relatives, and $\boldsymbol{1}_3$ is an 3-dimensional vector with elements of 1. Notice the difference between $\boldsymbol{1}_3$ here and d-dimensional $\boldsymbol{1}$, and the $\tilde{\boldsymbol{v}}$ and $\hat{\boldsymbol{v}}$ are different vectors. The constraints of $\boldsymbol{v}$ make it act as a qualified portfolio and within a distance ε from $\hat{\boldsymbol{v}}_t$.

Compared with the classical form of the increasing factor $\boldsymbol{v}^{\mathrm{T}}\tilde{\boldsymbol{s}}_{t+1}$ in PPT [6], $tr\left(\boldsymbol{V}\boldsymbol{\Psi}\tilde{\boldsymbol{S}}_{t+1}\right)$ can be considered as a generalized increasing factor. Because $tr\left(\boldsymbol{V}\boldsymbol{\Psi}\tilde{\boldsymbol{S}}_{t+1}\right)$ includes $\boldsymbol{\Psi}$ as the kernel to adjust the influence of different price prediction strategies. Strategy with the best performance $\tilde{\boldsymbol{s}}_{*,t+1}$ given it the largest influence, while other strategies $\{\tilde{\boldsymbol{s}}_{h,t+1}\}$ have the less influence and the magnitude of influence measured by their similarity to $\tilde{\boldsymbol{s}}_{*,t+1}$.

Inspired by the gradient projection principle [6] [8] [10] [31], when solving $\boldsymbol{v}_{t+1}$, the simplex constraint of $\boldsymbol{v}$ is firstly relaxed to only consider $\boldsymbol{1}^{\mathrm{T}}\boldsymbol{v} = 1$, and then the result is projected onto the simplex. And make $\boldsymbol{u} = \boldsymbol{v} - \hat{\boldsymbol{v}}_t$ here, then Equation (18) can be further converted into

$$\begin{aligned} &\boldsymbol{u}_{t+1} = \arg\max_{\boldsymbol{u}} tr\left(\boldsymbol{U}\boldsymbol{\Psi}\tilde{\boldsymbol{S}}_{t+1}^{\mathrm{T}}\right),\ \text{s.t}\ \mathbf{1}^{\mathrm{T}}\boldsymbol{u} = 0, \left\|\boldsymbol{u}\right\| \le \varepsilon \\ &\boldsymbol{U} = \boldsymbol{u}\mathbf{1}_{(3)}^{\mathrm{T}}, \boldsymbol{v}_{t+1} = \hat{\boldsymbol{v}}_t + \boldsymbol{u}_{t+1}, \end{aligned} \tag{19}$$

the reason for this simplification is that $\hat{\boldsymbol{v}}_t$ is fixed and $\mathbf{1}^{\mathrm{T}}\boldsymbol{u} = \mathbf{1}^{\mathrm{T}}\boldsymbol{v} - \mathbf{1}^{\mathrm{T}}\hat{\boldsymbol{v}}_t = 0$. Therefore, the optimization goal is now switching from $\boldsymbol{v}_{t+1}$ to the update increment $\boldsymbol{u}_{t+1}$.

3.3. Solution Algorithm

In this subsection, the solution algorithm of CPP is introduced in detail, which has briefly concluded in Proposition 1. It is worth noting that our solution is suboptimal, not only because there is a certain bias in estimating the future with historical data but also to avoid over-fitting. So it's not necessary to get the optimal solution.

Proposition 1. If $\left(\boldsymbol{I} - \left(\frac{1}{d}\right)\mathbf{1}\mathbf{1}^{\mathrm{T}}\right)\tilde{\boldsymbol{S}}_{t+1}\boldsymbol{\Psi}\mathbf{1}_{(3)} \neq 0$, the unique solution of Equation (19) is

$$\boldsymbol{u}_{t+1} = \frac{\varepsilon\left(\boldsymbol{I} - \frac{1}{d}\mathbf{1}\mathbf{1}^{\mathrm{T}}\right)\tilde{\boldsymbol{S}}_{t+1}\boldsymbol{\Psi}\mathbf{1}_{(3)}}{\left\|\left(\boldsymbol{I} - \frac{1}{d}\mathbf{1}\mathbf{1}^{\mathrm{T}}\right)\tilde{\boldsymbol{S}}_{t+1}\boldsymbol{\Psi}\mathbf{1}_{(3)}\right\|}, \tag{20}$$

note that if $\left(\boldsymbol{I} - \frac{1}{d}\mathbf{1}\mathbf{1}^{\mathrm{T}}\right)\tilde{\boldsymbol{S}}_{t+1}\boldsymbol{\Psi}\mathbf{1}_{(3)} = 0$, we make $\boldsymbol{u}_{t+1} = 0$.

Proof. The first step is to prove that $\boldsymbol{u}_{t+1}$ satisfies all constraints in Equation (19), that is

$$\left\|\boldsymbol{u}_{t+1}\right\| = 1 \tag{21}$$

$$\begin{aligned} \mathbf{1}^{\mathrm{T}}\boldsymbol{u}_{t+1} &= \frac{\varepsilon\mathbf{1}^{\mathrm{T}}\left(\boldsymbol{I} - \frac{1}{d}\mathbf{1}\mathbf{1}^{\mathrm{T}}\right)\tilde{\boldsymbol{S}}_{t+1}\boldsymbol{\Psi}\mathbf{1}_{(3)}}{\left\|\left(\boldsymbol{I} - \frac{1}{d}\mathbf{1}\mathbf{1}^{\mathrm{T}}\right)\tilde{\boldsymbol{S}}_{t+1}\boldsymbol{\Psi}\mathbf{1}_{(3)}\right\|} \\ &= \frac{\varepsilon\left(\mathbf{1}^{\mathrm{T}} - \frac{1}{d}\left(\mathbf{1}^{\mathrm{T}}\mathbf{1}\right)\mathbf{1}^{\mathrm{T}}\right)\tilde{\boldsymbol{S}}_{t+1}\boldsymbol{\Psi}\mathbf{1}_{(3)}}{\left\|\left(\boldsymbol{I} - \frac{1}{d}\mathbf{1}\mathbf{1}^{\mathrm{T}}\right)\tilde{\boldsymbol{S}}_{t+1}\boldsymbol{\Psi}\mathbf{1}_{(3)}\right\|} \\ &= 0 \end{aligned} \tag{22}$$

So $\boldsymbol{u}_{t+1}$ satisfies the two constraints. The second step is to prove that the optimization problem in Equation (19) maximizes at $\boldsymbol{u}_{t+1}$. By contradiction we suppose that there exists $\hat{\boldsymbol{u}}$ that satisfies all constraints and

$$tr\left(\hat{\boldsymbol{U}}\boldsymbol{\Psi}\tilde{\boldsymbol{S}}_{t+1}^{\mathrm{T}}\right) > tr\left(\boldsymbol{U}_{t+1}\boldsymbol{\Psi}\tilde{\boldsymbol{S}}_{t+1}^{\mathrm{T}}\right), \tag{23}$$

where $\hat{\boldsymbol{U}} = \hat{\boldsymbol{u}}\mathbf{1}_3$, $\boldsymbol{U}_{t+1} = \boldsymbol{u}_{t+1}\mathbf{1}_3$.

On the one hand, the right side of the Equation (23) can be converted to

$$tr\left(\boldsymbol{U}_{t+1}\boldsymbol{\Psi}\tilde{\boldsymbol{S}}_{t+1}^{\mathrm{T}}\right) = tr\left(\boldsymbol{u}_{t+1}\mathbf{1}_3^{\mathrm{T}}\boldsymbol{\Psi}\tilde{\boldsymbol{S}}_{t+1}^{\mathrm{T}}\right) = tr\left(\mathbf{1}_3^{\mathrm{T}}\boldsymbol{\Psi}\tilde{\boldsymbol{S}}_{t+1}^{\mathrm{T}}\boldsymbol{u}_{t+1}\right) = \mathbf{1}_3^{\mathrm{T}}\boldsymbol{\Psi}\tilde{\boldsymbol{S}}_{t+1}^{\mathrm{T}}\boldsymbol{u}_{t+1} \tag{24}$$

Note that $\mathbf{1}_3^{\mathrm{T}}\boldsymbol{\Psi}\tilde{\boldsymbol{S}}_{t+1}^{\mathrm{T}}\boldsymbol{u}_{t+1}$ is a scalar.

Then we substitute $\boldsymbol{u}_{t+1}$ into the scalar

$$\begin{aligned}\mathbf{1}_3^{\mathrm{T}}\boldsymbol{\Psi}\tilde{\boldsymbol{S}}_{t+1}^{\mathrm{T}}\boldsymbol{u}_{t+1} &= \frac{\varepsilon\mathbf{1}_3^{\mathrm{T}}\boldsymbol{\Psi}\tilde{\boldsymbol{S}}_{t+1}^{\mathrm{T}}\left(\boldsymbol{I}-\frac{1}{d}\mathbf{1}\mathbf{1}^{\mathrm{T}}\right)\tilde{\boldsymbol{S}}_{t+1}\boldsymbol{\Psi}\mathbf{1}_{(3)}}{\left\|\left(\boldsymbol{I}-\frac{1}{d}\mathbf{1}\mathbf{1}^{\mathrm{T}}\right)\tilde{\boldsymbol{S}}_{t+1}\boldsymbol{\Psi}\mathbf{1}_{(3)}\right\|} \\ &= \frac{\varepsilon\mathbf{1}_3^{\mathrm{T}}\boldsymbol{\Psi}\tilde{\boldsymbol{S}}_{t+1}^{\mathrm{T}}\left(\boldsymbol{I}-\frac{1}{d}\mathbf{1}\mathbf{1}^{\mathrm{T}}\right)^2\tilde{\boldsymbol{S}}_{t+1}\boldsymbol{\Psi}\mathbf{1}_{(3)}}{\left\|\left(\boldsymbol{I}-\frac{1}{d}\mathbf{1}\mathbf{1}^{\mathrm{T}}\right)\tilde{\boldsymbol{S}}_{t+1}\boldsymbol{\Psi}\mathbf{1}_{(3)}\right\|} \\ &= \varepsilon\left\|\left(\boldsymbol{I}-\frac{1}{d}\mathbf{1}\mathbf{1}^{\mathrm{T}}\right)\tilde{\boldsymbol{S}}_{t+1}\boldsymbol{\Psi}\mathbf{1}_{(3)}\right\|\end{aligned} \tag{25}$$

The second equation is derived from the idempotent of $\left(\boldsymbol{I}-\frac{1}{d}\mathbf{1}\mathbf{1}^{\mathrm{T}}\right)$.

On the other hand, the left side of the Equation (23) can be converted to

$$\begin{aligned}tr\left(\hat{\boldsymbol{U}}\boldsymbol{\Psi}\tilde{\boldsymbol{S}}_{t+1}^{\mathrm{T}}\right) &= \mathbf{1}_3^{\mathrm{T}}\boldsymbol{\Psi}\tilde{\boldsymbol{S}}_{t+1}^{\mathrm{T}}\hat{\boldsymbol{u}} \\ &= \mathbf{1}_3^{\mathrm{T}}\boldsymbol{\Psi}\tilde{\boldsymbol{S}}_{t+1}^{\mathrm{T}}\left(\boldsymbol{I}-\frac{1}{d}\mathbf{1}\mathbf{1}^{\mathrm{T}}\right)\hat{\boldsymbol{u}} \\ &\le \left\|\mathbf{1}_3^{\mathrm{T}}\boldsymbol{\Psi}\tilde{\boldsymbol{S}}_{t+1}^{\mathrm{T}}\left(\boldsymbol{I}-\frac{1}{d}\mathbf{1}\mathbf{1}^{\mathrm{T}}\right)\right\|\left\|\hat{\boldsymbol{u}}\right\|\end{aligned} \tag{26}$$

The inequality is derived from Cauchy-Schwarz inequality.

Take Equation (23), Equation (25) and Equation (26) into consideration, we have

$$\varepsilon\left\|\left(\boldsymbol{I}-\frac{1}{d}\mathbf{1}\mathbf{1}^{\mathrm{T}}\right)\tilde{\boldsymbol{S}}_{t+1}\boldsymbol{\Psi}\mathbf{1}_{(3)}\right\| < \left\|\mathbf{1}_3^{\mathrm{T}}\boldsymbol{\Psi}\tilde{\boldsymbol{S}}_{t+1}^{\mathrm{T}}\left(\boldsymbol{I}-\frac{1}{d}\mathbf{1}\mathbf{1}^{\mathrm{T}}\right)\right\|\left\|\hat{\boldsymbol{u}}\right\| \tag{27}$$

Hence, we can deduce $\left\|\hat{\boldsymbol{u}}\right\| < \varepsilon$. This contradicts $\left\|\hat{\boldsymbol{u}}\right\| \le \varepsilon$. It is proved that the optimization problem in Equation (19) obtain the maximum at $\boldsymbol{u}_{t+1}$

Finally, we prove that the solution $\boldsymbol{u}_{t+1}$ is unique. If $\boldsymbol{u}_{t+1}$ is not the only solution, then there must be another optimal solution $\boldsymbol{u}_* \ne \boldsymbol{u}_{t+1}$, and

$$\mathbf{1}_3^{\mathrm{T}}\boldsymbol{\Psi}\tilde{\boldsymbol{S}}_{t+1}^{\mathrm{T}}\boldsymbol{u}_{t+1} = tr\left(\boldsymbol{U}_{t+1}\boldsymbol{\Psi}\tilde{\boldsymbol{S}}_{t+1}^{\mathrm{T}}\right) = tr\left(\boldsymbol{U}_*\boldsymbol{\Psi}\tilde{\boldsymbol{S}}_{t+1}^{\mathrm{T}}\right) = \mathbf{1}_3^{\mathrm{T}}\boldsymbol{\Psi}\tilde{\boldsymbol{S}}_{t+1}^{\mathrm{T}}\boldsymbol{u}_* \tag{28}$$

This shows that $\boldsymbol{u}_* \nparallel \boldsymbol{u}_{t+1}$. So the Cauchy-Schwarz inequality is strict

$$\mathbf{1}_3^{\mathrm{T}}\boldsymbol{\Psi}\tilde{\boldsymbol{S}}_{t+1}^{\mathrm{T}}\boldsymbol{u}_* = \mathbf{1}_3^{\mathrm{T}}\boldsymbol{\Psi}\tilde{\boldsymbol{S}}_{t+1}^{\mathrm{T}}\left(\boldsymbol{I}-\frac{1}{d}\mathbf{1}\mathbf{1}^{\mathrm{T}}\right)\boldsymbol{u}_* < \left\|\mathbf{1}_3^{\mathrm{T}}\boldsymbol{\Psi}\tilde{\boldsymbol{S}}_{t+1}^{\mathrm{T}}\left(\boldsymbol{I}-\frac{1}{d}\mathbf{1}\mathbf{1}^{\mathrm{T}}\right)\right\|\left\|\boldsymbol{u}_*\right\| \tag{29}$$

According to Equation (25) and Equation (29), we obtain $\left\|\boldsymbol{u}_*\right\| > \varepsilon$. This contradicts the constraint $\left\|\boldsymbol{u}_*\right\| < \varepsilon$.

To sum up, we can get that $\boldsymbol{u}_{t+1}$ is the optimal and unique solution of optimization problem in Equation (19). □

Regarding *Proposition* 1, the update increment

$$\boldsymbol{u}_{t+1} = \mathcal{A}_\varepsilon\left(\left(\boldsymbol{I}-\frac{1}{d}\mathbf{1}\mathbf{1}^{\mathrm{T}}\right)\tilde{\boldsymbol{S}}_{t+1}\boldsymbol{\Psi}\mathbf{1}_{(3)}\right) = \mathcal{A}_\varepsilon\left(\left(\boldsymbol{I}-\frac{1}{d}\mathbf{1}\mathbf{1}^{\mathrm{T}}\right)\tilde{\boldsymbol{S}}_{t+1}\boldsymbol{\psi}\right), \tag{30}$$

where $\mathcal{A}_\varepsilon$ is a mapping projected onto the ε-Euclidean ball. Compared with Equation (17), in order to satisfy the constraint conditions in Equation (19), $\boldsymbol{u}_{t+1}$ adds two operators on the basis of $\Delta\boldsymbol{v}_{t+1}$. Thus, this is also explains why the update increment of the portfolio is represented as Equation (17).

Then, the portfolio $\hat{\boldsymbol{v}}_{t+1}$ on the next period is shown as follows:

$$\begin{aligned} \boldsymbol{v}_{t+1} &= \hat{\boldsymbol{v}}_t + \boldsymbol{u}_{t+1} \\ \hat{\boldsymbol{v}}_{t+1} &= \arg\min_{\boldsymbol{v}\in\Delta_d} \left\| \boldsymbol{v} - \boldsymbol{v}_{t+1} \right\|^2. \end{aligned} \tag{31}$$

The complete CPP system is outlined in Algorithm 1. CPP is a fast algorithm because it only uses ordinary matrix calculation without any iterative calculation, which significantly reduces the operation time.

4. Experiments

4.1. Data Sets and Comparison Approaches

In this subsection, in order to comprehensively assess the performance of systems, a large number of experiments were carried out on four data sets, namely NYSE(N), DJIA, SP500 and HS300. In fact, they contain the daily price relatives of assets, originating from the New York Stock Exchange, Dow Jones Industrial Average, Standard & Pool 500 and China Stock Index 300, respectively. These data sets have larger assets scales and long time spans. So they can be used to assess the investing performance of systems. The details of these data sets are introduced in Table 1.

Table 1. Summary of 4 benchmark data sets from real-world financial market.

Dataset	Region	Time	Periods	Stocks
NYSE(N)	US	1/1/1985-30/6/2010	6431	23
DJIA	US	14/1/2001-14/1/2003	507	30
SP500	US	2/1/1998-31/1/2003	1276	25
HS300	CN	21/1/2006-16/10/2017	421	44

Algorithm 1. The whole CPP system.

Input: Given time window size ω, parameters ϵ and $\{\sigma_h^2\}_{h=1}^3$, the price predictions $\{\tilde{\mathbf{s}}_{h,t-k}\}_{k=0}^{\omega-1}$, the price relatives$\{\mathbf{s}_{t-k}\}_{k=0}^{\omega-1}$, and the current portfolio $\hat{\mathbf{v}}_t$.

Compute the quantified portfolios $\{\tilde{\mathbf{v}}_{h,t-k}\}_{k=0}^{\omega-1}$ by Eq.(15).
Compute the input of novel RBF system $\tilde{\mathbf{s}}_{*,t+1}$ by Eq.(16).
Compute $\{\psi_h\}_{h=1}^3$ by Eq.(17).
if $(\mathbf{I} - (\frac{1}{d})\mathbf{1}\mathbf{1}^\top)\tilde{\mathbf{S}}_{t+1}\boldsymbol{\Psi}\mathbf{1}_{(3)} \neq 0$ **then**.
Let $\mathbf{u}_{t+1} = 0$
else
Compute $\mathbf{u}_{t+1} = \frac{\epsilon(\mathbf{I}-\frac{1}{d}\mathbf{1}\mathbf{1}^\top)\tilde{\mathbf{S}}_{t+1}\boldsymbol{\Psi}\mathbf{1}_{(3)}}{\|(\mathbf{I}-\frac{1}{d}\mathbf{1}\mathbf{1}^\top)\tilde{\mathbf{R}}_{t+1}\boldsymbol{\Psi}\mathbf{1}_{(3)}\|}$.
end if
Compute $\mathbf{v}_{t+1} = \hat{\mathbf{v}}_t + \mathbf{u}_{t+1}$
Obtain the portfolio $\hat{\mathbf{v}}_{t+1}$ on $t+1$ period by Eq(31).

Output: The portfolio $\hat{\mathbf{v}}_{t+1}$ on $t+1$ period.

Six commonly used PS systems are introduced, namely RMR, OLMAR, PPT, TRLR [32], SSPO [33] and AICTR [34], to compete with CPP that we proposed. A detailed descriptions of these systems are as follow.

1) RMR: RMR uses L_1-median to make price prediction as described in Section 2.2.

2) OLMAR: OLMAR uses the moving averages to make price prediction, which are described in Section 2.2.

3) PPT: PPT is an aggressive strategy that uses the maximum values of different assets to make price prediction as mentioned in Section 2.2.

4) TRLR: TRLR [32] is a novel trend representation strategy. It exploits weighted ridge regression to represent the price trend pattern with time t as a variable, which improves the efficiency of the price prediction.

5) SSPO: SSPO [33] is an aggressive strategy and concentrates wealth on a small number of assets by taking advantage of the inherent sparsity of assets to maximize the final CW.

6) AICTR: AICTR [34] is a composite trend tracking system using Gaussian basis function.

In order to ensure the performance of these systems, the parameter settings of these systems are consistent with the default settings in the original paper [6] [8] [10] [32] [33] [34]. RMR: $\omega = 5$, $\varepsilon = 5$; OLMAR: $\nu = 0.5$, $\varepsilon = 10$; PPT: $\omega = 5$, $\varepsilon = 100$; TRLR: $\omega = 5$, $q_1 = 0.1$, $\lambda = 0.7$, $\sigma = 0.3$, $\eta = 40000$; SSPO: $\omega = 5$, $\gamma = 0.01$, $\lambda = 0.5$, $\eta = 0.005$, $\zeta = 500$; AICTR: $\omega = 5$, $\sigma_h^2 = 0.0025$, $\varepsilon = 1000$. Note that for consistency, all time window sizes are set to $\omega = 5$. In the experiments, the portfolio vector is initialized to $\boldsymbol{v}_1 = (1/d)\mathbf{1}$.

In general, the parameters of CPP are determined based on the results of final cumulative wealth (CW), operating in the same way as previous studies. The calculation of final CW is described in detail in Section 2.1. First, we set the window size $\omega = 5$, which is widely used and consistent with other systems. Secondly, we change one parameter to fix the other parameters for the experiments. Since ε is the updating strength, it is roughly estimated to be larger value, while σ_h^2 is a parameter used to evaluate the difference between two portfolios, it should be a small value. On the one hand, we firstly set $\omega = 5$, $\varepsilon = 1400$, and then set σ_h^2 change between 0.0007 and 1.0012. According to the results in **Figure 1**, the investing performance of CPP around $\sigma_h^2 = 0.0008$ is stable and good. On the other hand, we firstly set $\omega = 5$, $\sigma_h^2 = 0.0008$ and then make ε change between 1200 and 1700. The results are shown in **Figure 2** and we know that CPP is stable and good around $\varepsilon = 1400$. Therefore, the parameters of CPP are set as: $\sigma_h^2 = 0.0008$, $\varepsilon = 1400$.

4.2. Experimental Results

In this paper, a scheme containing seven evaluation indicators are designed to assess the performance of different systems and achieve the most excellent results. These seven indicators can be roughly divided into three categories, namely investing performance, risk metrics and application issues. Investing performance

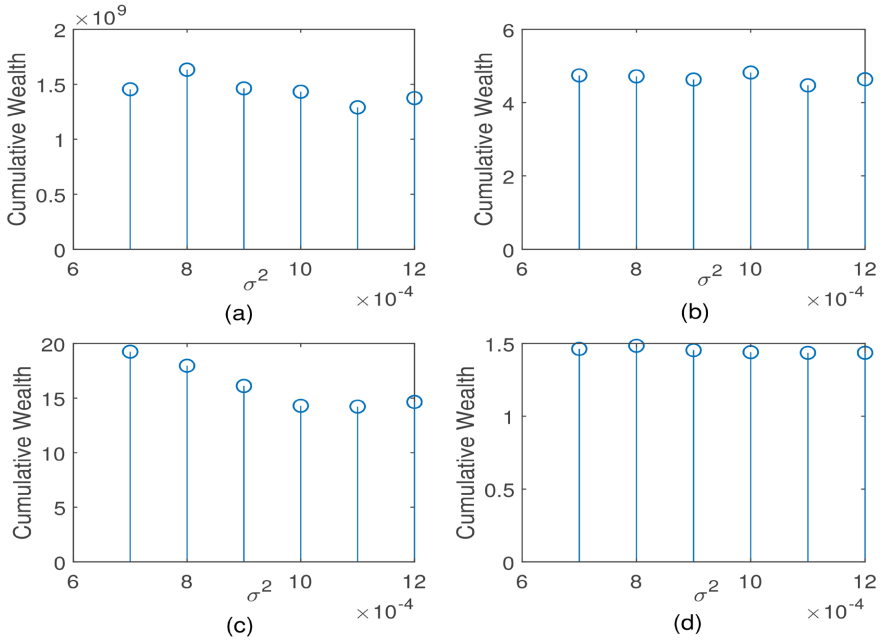

Figure 1. Final CWs of CPP in regard to σ_h^2 on four data sets (fixed $\omega = 5$, $\varepsilon = 1400$). (a) NYSE(N), (b) DJIA, (c) SP500, (d) HS300.

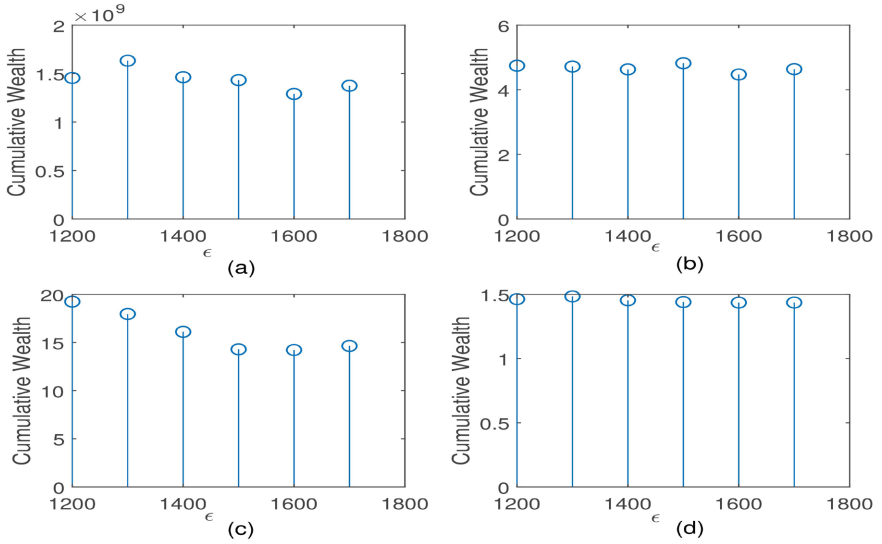

Figure 2. Final CWs of CPP in regard to ε on four data sets (fixed $\omega = 5$, $\sigma_h^2 = 0.0008$). (a) NYSE(N), (b) DJIA, (c) SP500, (d) HS300.

includes CW, mean excess return (MER) and α Factors. Risk metrics consist of sharpe ratio (SR) and information ratio (IR). As for application issues, we chose transaction cost and running times to assess them. Those indications will be discussed in the following subsection.

4.2.1. Investing Performance

1) CW: The final CWs are the primary consideration in evaluating a system. Without taking transaction into account, the results of CWs for various systems

mentioned in Section 4.1 are shown in Table 2. CPP outperforms seven commonly used systems on three data sets and ranks third on NYSE(N). For example, CPP(4.74, 18.05) is significantly higher than PPT(3.08, 10.78), TRLR(2.71, 13.17) and OLMAR(1.16, 9.59), respectively. In addition, DJIA is a challenging data set because many systems do not perform well in this data set, such as PPT, and OLMAR. But CPP can reach a value of 4.74, which is 53.90% higher than PPT. These results shows that CPP is an effective PS system and can accumulate more wealth in the real financial market.

In order to show the superiority of the system CPP, the CWs of each system on DJIA is plotted in Figure 3. By observing the Figure 3, the excellent investing performance of CPP can be shown more intuitively.

2) MER: Return is a financial term that describes the proportion of wealth by a PS system gained or lost over one investing period. In this paper, the daily return

Table 2. Final CWs and MERs of different PS systems on 4 data sets.

System	NYSE(N)		DJIA		SP500		HS300	
	CW	MER	CW	MER	CW	MER	CW	MER
RMR	3.25E+8	0.0032	2.67	0.0029	8.28	0.0019	1.35	0.0001
OLMAR	4.69E+8	0.0032	1.16	0.0012	9.59	0.0020	1.20	0.0001
PPT	**2.89E+9**	**0.0036**	3.08	0.0031	10.78	0.0022	1.09	−0.0004
TRLR	2.29E+9	0.0035	2.71	0.0030	13.17	0.0023	1.34	0.0001
SSPO	1.62E+9	0.0035	3.68	0.00036	16.97	0.0025	1.08	−0.0004
AICTR	7.66E+8	0.0033	4.17	0.0038	14.22	0.0024	1.42	0.0003
CPP	1.67E+9	0.0034	**4.74**	**0.0041**	**18.05**	**0.0025**	**1.48**	**0.0004**

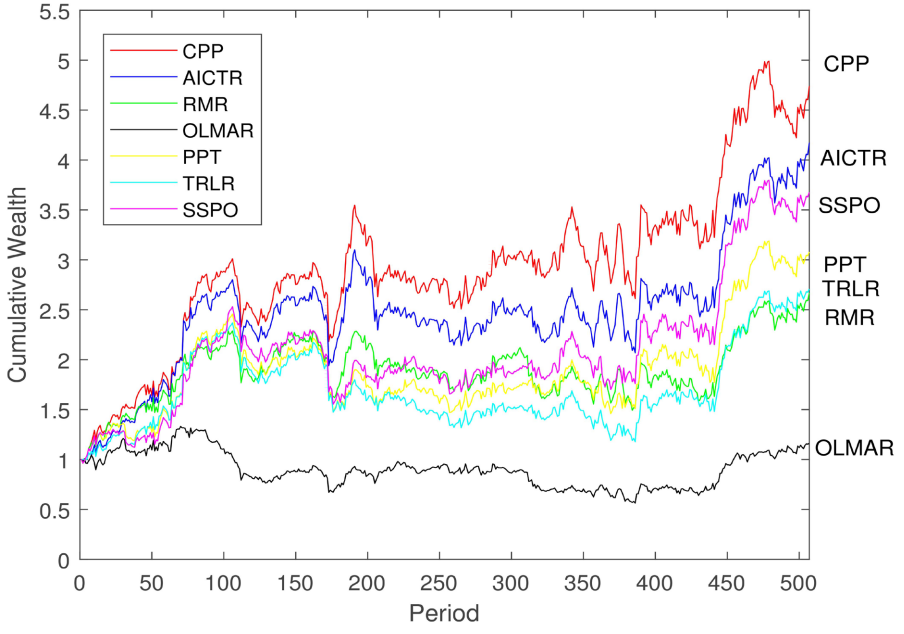

Figure 3. Daily *CWs* of different PS systems on DJIA.

on the tth period is $r_t = \hat{\boldsymbol{v}}_t^{\mathrm{T}} \boldsymbol{s}_t - 1$. MER [35] is an indicator that computes the long-term average daily excess return of attended PS systems

$$\mathrm{MER} = \overline{r}_s - \overline{r}_m = \frac{1}{n}\sum_{t=1}^{n}\left(r_{s,t} - r_{m,t}\right), \tag{32}$$

where $r_{s,t}$ and $r_{m,t}$ present the daily returns of attended PS system and the market baseline on the tth period, respectively. Note that, the UBAH system is defined as the market baseline.

The MER results from various PS systems are described in **Table 2**. CPP obtains the largest MER on three data sets and ranks third on NYSE(N). For instance, CPP(0.0041, 0.0004) is significantly higher than PPT(0.0031, −0.0004), OLMAR(0.0012, 0.0001) and TRLR(0.0030, 0.0001) on DJIA and HS300 respectively. In addition, a small MER gap is likely to produce a lager CW gap in the long-term. Therefore, the above results demonstrate that CPP can achieve an outstanding investing performance.

3) α Factor: MER measures the investing performance of a PS system without considering market risks. However, in the real financial market, the volatility of the market will undoubtedly affect the performance of assets. Capital asset pricing model(CAPM) [36] points out that the expected return sources of PS systems can be divided into two parts: the first part comes from the market return, and the second comes from the inherent excess return, also called α Factor [37] [38]. Therefore, α Factor able to evaluate the investing performance of different PS systems:

$$E\left(r_s\right) = \alpha + \beta E\left(r_m\right),\ \hat{\beta} = \frac{\hat{c}\left(r_s, r_m\right)}{\hat{s}^2\left(r_m\right)},\ \hat{\alpha} = \overline{r}_s - \hat{\beta}\overline{r}_m \tag{33}$$

where $E(\cdot)$ is the mathematical expectation of the sample data, and $\hat{c}(\cdot)$ and $\hat{s}(\cdot)$ are covariance matrix and standard deviation calculated from the daily return of n trading days, respectively.

The α Factor results from all PS systems mentioned are presented in **Table 3**. CPP achieved the highest α on three data sets and ranked second on the NYSE(N). For example, CPP (0.0042, 0.0002) achieves a higher α, compared

Table 3. α Factors (with p-Values of t-tests) of different PS systems on four data sets.

System	NYSE(N)		DJIA		SP500		HS300	
	α Factor	p-Value	α Factor	p-Value	α Factor	p-Value	α Factor	p-Value
RMR	0.0031	<0.0001	0.0030	0.0054	0.0018	0.0102	−4.5e−5	0.5261
OLMAR	0.0031	0.0000	0.0013	0.1366	0.0019	0.0082	−0.0003	<0.0001
PPT	**0.0035**	<0.0001	0.0034	0.0024	0.0020	0.0065	−0.0005	0.7465
TRLR	**0.0035**	<0.0001	0.0031	0.0043	0.0022	0.0039	0.0001	<0.0001
SSPO	0.0034	<0.0001	0.0037	0.00009	0.0024	0.0019	−0.0005	<0.0001
AICTR	0.0032	<0.0001	0.0039	<0.0001	0.0022	0.0027	6.8e−5	0.4638
CPP	0.0034	<0.0001	**0.0042**	<0.0001	**0.0024**	<0.0001	**0.0002**	<0.0001

with RMR(0.0030, −4.5E−5), PPT(0.0034, −0.0005), OLMAR(0.0013, −0.0003) and TRLR(0.0031, 0.0001) on DJIA and HS300, respectively. The above results show that CPP is still able to achieve higher inherent excess return in the face of market volatility. In addition, the statistical t-test is used to determine whether α is significantly lager than 0, proving that the inherent excess return is not achieved by luck. The results of p-value presented in **Table 3** and the α of CPP is significantly lager than 0 at a high confidence level of 99% (with all p-values < 0.01). It shows that CPP achieves good inherent excess returns and the obtained results are not the result of luck.

4.2.2. Risk Metrics

1) Sharpe Ratio: In the real financial market, risks and returns coexist, and high excess returns often mean high risks. Wise investors will balance returns and risks before investing. Sharpe proposed SR [36] [39] to measure risk-adjusted return

$$\mathrm{SR} = \frac{\overline{r}_s - r_f}{\hat{s}\left(r_s\right)} \tag{34}$$

where r_f is the return of risk-free assets, and $\overline{r}_s$ and $\hat{s}\left(r_s\right)$ are the average return and the standard deviation calculated from the daily return of n periods respectively. Note that, this article don't consider risk-free assets. So let $r_f = 0$.

The results of SR for various PS systems are presented in **Table 4**. CPP stands out among commonly used systems and achieves the highest SR on all data sets. For example, CPP(0.1076, 0.0599) achieves the highest SR compared to AICTR (0.0995, 0.0555), OLMAR(0.0252, 0.0353), and SSPO(0.0919, 0.0192) on DJIA and HS300 respectively. The above results prove that CPP has an excellent ability to balance return and risk compared with commonly used systems.

2) Information Ratio: Unlike SR, IR [40] does not directly measure the risk-adjusted excess return of a system, but measures it compared to the Market

$$\mathrm{IR} = \frac{\overline{r}_s - \overline{r}_m}{\hat{s}\left(r_s - r_m\right)} \tag{35}$$

Table 4. SRs and IRs of different PS systems on four data sets.

System	NYSE(N)		DJIA		SP500		HS300	
	SR	IR	SR	IR	SR	IR	SR	IR
RMR	0.1033	0.0953	0.0763	0.1092	0.0600	0.0678	0.0473	−0.0061
OLMAR	0.1050	0.0970	0.0252	0.0457	0.0682	0.0700	0.0353	0.0001
PPT	**0.1087**	0.1008	0.0821	0.1176	0.0699	0.0728	0.0207	−0.0255
TRLR	0.1086	0.1004	0.0750	0.1091	0.0738	0.0777	0.0463	0.0001
SSPO	1.1060	0.0035	00919	0.00036	0.0791	0.0025	0.0192	0.0079
AICTR	0.1056	0.0979	0.0995	0.1364	0.0763	0.0810	0.0555	0.0181
CPP	**0.1087**	**0.1012**	**0.1076**	**0.1471**	**0.0818**	**0.0872**	**0.0599**	**0.0259**

The results of IR are presented in Table 4. CPP obtains the highest IR among commonly used systems on all data sets. For example, CPP(0.1012, 0.1417) outperforms AICTR(0.0979, 0.1364), PPT(0.1008,0.1176), OLMAR(0.0970, 0.0457), RMR(0.0953, 0.1092) and SSPO(0.0979, 0.1304) on NYSE(N) and DJIA respectively. Therefore, CPP is a robust system, which can obtain good excess returns and able to control risks effectively.

4.2.3. Application Issues

1) Transaction Cost: In the real-world financial environment, the transaction cost is a problem that cannot be ignored. Suppose that the transaction cost rate required to update the portfolio denoted as $\gamma \in (0,1)$. The proportional transaction cost model [8] [10] [41] assumes that the final CW at the beginning of the tth period can be expressed as

$$W_n^{\gamma} = W_0 \prod_{t=1}^{n} \left[\left(\hat{\boldsymbol{v}}_t^{\mathrm{T}} \boldsymbol{s}_t \right) \times \left(1 - \frac{\gamma}{2} \sum_{i=1}^{d} \left| \hat{\boldsymbol{v}}_t^i - \tilde{\boldsymbol{v}}_{t-1}^{(i)} \right| \right) \right]$$

$$\tilde{\boldsymbol{v}}_{t-1}^{(i)} = \frac{\hat{\boldsymbol{v}}_{t-1}^{(i)} * \boldsymbol{s}_{t-1}^{(i)}}{\hat{\boldsymbol{v}}_{t-1}^{\mathrm{T}} \boldsymbol{s}_{t-1}}$$

where $\tilde{\boldsymbol{v}}_{t-1}^{(i)}$ represents the adjusted portfolio of the tth asset at the end of the $(t-1)$ th period and let $\tilde{\boldsymbol{v}}_0 = 0$. $\left(\frac{\gamma}{2} \right) \sum_{i=1}^{d} \left| \hat{\boldsymbol{v}}_t^i - \tilde{\boldsymbol{v}}_{t-1}^{(i)} \right|$ stands the proportional transaction cost used to update portfolios from the adjusted portfolio to the next portfolio $\tilde{\boldsymbol{v}}_t$.

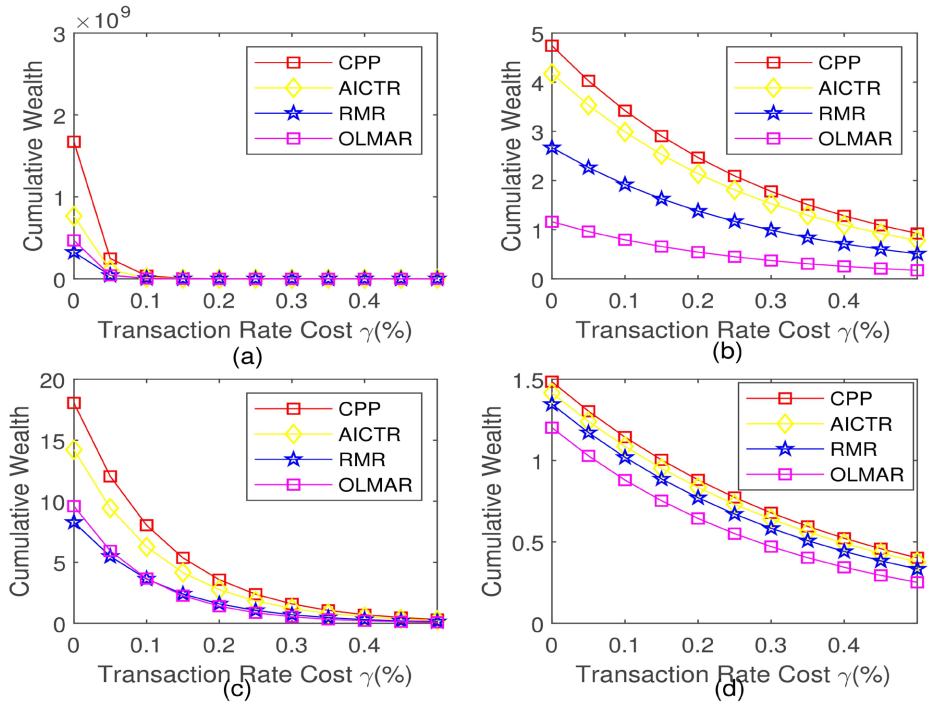

Figure 4. Final CWs of different PS systems in regard to transaction cost rate γ on four data sets. (a) NYSE(N), (b) DJIA, (c) SP300, (d) HS300.

In the case of considering transaction costs, in order to better assess the investment performance of CPP, we let γ change between 0% and 0.5% and carry out experiments to calculate the final CWs of different commonly used systems. The results are presented in **Figure 4**. CPP achieves the highest CW on all data sets when the transaction cost rate γ fluctuates between 0% and 0.15%. In addition, even when γ reaches a high value ($0.15\% \le \gamma \le 0.5\%$), CPP still outperforms other PS systems on three data sets. Therefore, it shows that CPP can bear moderate transaction costs and can be applied in real world financial markets.

2) Running Times: Running Time is an important indicator to judge whether a system can be applied in a large-scale and time-limiting environment, such as High-Frequency Trading (HFT) [42]. We use a regular computer equipped an Intel Core i5-8250U CPU and 8GB DDR4 2400 MHZ memory card to perform CPP in the experiments. The average running times of CPP for one trading period are 1.751e−4, 1.876e−4, 1.936e−4 and 1.876e−4 on NYSE(N), DJIA, SP500 and HS300, respectively. Therefore, CPP has good computational efficiency and can be applied in large-scale financial markets.

5. Conclusion

In this paper, we proposed a new CPP system based on IMQ radial basis function with an integration of three different aggressive and moderate strategies for effective and robust PS. Instead of using a traditional GA function, here we chose a more stable and accurate function that is IMQ for the novel RBF system, which centers on multiple strategies. With regard to portfolio update, different from the traditional increasing factor, we propose a generalized growth factor based on a kernel and trace operation. And CPP is fast and can be applied in larger scale and limited time financial environment. Extensive experiments are performed on 4 worldwide benchmark data sets to indicate that CPP can effectively integrate the advantages of different strategies and it was proved to be effective in PS. On the one hand, in most cases CPP outperforms other commonly used systems in performance indicators CW, MER and α Factor. On the other hand, CPP achieves the highest SR and IR compared with other systems. The results show that CPP has not only excellent investing performance but also good risk control ability. In addition, CPP can withstand reasonable transaction costs and fast operation, which have to be considered in the real financial market. In conclusion, CPP is an efficient and robust PS system and deserves further investigation. Of course, the CPP system has its own shortcomings. On one hand, the problem of reducing transaction cost was not considered at the initial stage of modeling. On other hand, this paper considers only the three strategies. In the future, we can improve the performance of the system from these two aspects.

6. Acknowledgements

Thanks to Jinan University for the resources provided, and to tutors for their

valuable advice on this manuscript. This research is supported by the National Natural Science Foundation of China under Grants 61703182, the Science and Technology Planning Project of Guangzhou, China under Grants 202102021173 and the Fundamental Research Funds for the Central Universities under Grants 21617347.

Conflicts of Interest

The author declares no conflicts of interest regarding the publication of this paper.

References

[1] Markowitz, H.M. (1952) Portfolio Selection. *Journal of Finance*, **7**, 77-91. https://doi.org/10.1111/j.1540-6261.1952.tb01525.x

[2] Kelly Jr., J. (1956) A New Interpretation of Information Rate. *Bell System Technical Journal*, **35**, 917-926. https://doi.org/10.1002/j.1538-7305.1956.tb03809.x

[3] Finkelstein, M. and Whitley, R. (1981) Optimal Strategies for Repeated Games. *Advance in Applied Probability*, **13**, 415-428. https://doi.org/10.2307/1426692

[4] Wilder, W. (2012) The ADAM Theory of Markets. *Shanxi Peoples's Publishing House*.

[5] Li, B. and Hoi, S.C.H. (2014) Online Portfolio Selection: A Survey. *ACM Computing Surveys*, **46**, Article No. 35. https://doi.org/10.1145/2512962

[6] Lai, Z.R., Dai, D.Q., Ren, C.X. and Huang, K.-K. (2018) A Peak Price Tarcking-Based Learning System for Portfolio Selection. *IEEE Transactions Neural Newtworks and Learning Systems*, **29**, 2823-2832.

[7] Borodin, A., EL-Yaniv, R. and Gogan, V. (2004) Can We Learn to Beat the Best Stock. *Journal of Artificial Intelligence Research*, **21**, 579-694. https://doi.org/10.1613/jair.1336

[8] Huang, D.-J., Zhou, J.-L. and Li, B. (2016) Robust Median Reversion Strategy for Online PS. *IEEE Transactions Neural Newtworks and Learning Systems*, **28**, 2480-2493. https://doi.org/10.1109/TKDE.2016.2563433

[9] Li, B., Hoi, S.C.H. and Zhao, P.-L. (2013) Confidence Weighted Mean Reversion Strategy for Online PS. *ACM Transactions on Knowledge Discovery from Data*, **7**, Article No. 4. https://doi.org/10.1145/2435209.2435213

[10] Li, B., Hoi, S.C.H., Sahoo, D. and Liu, Z.-Y. (2015) Moving Average Reversion Strategy for Online Portfolio Selection. *Artificial Intelligence*, **222**, 104-123. https://doi.org/10.1016/j.artint.2015.01.006

[11] Gyorfi, L., Urban, A. and Vajda, I. (2007) Kernel-Based Semi-Log-Optimal Empirical Empirical Portfolio Selection Strategies. *International Journal Theoretical and Applied Finance*, **10**, 505-516. https://doi.org/10.1142/S0219024907004251

[12] Gyorfi, L., Lugosi, G. and Udina, F. (2006) Nonparametric Kernel-Based Sequential Investment Strategies. *Mathematical Finance*, **16**, 337-357. https://doi.org/10.1111/j.1467-9965.2006.00274.x

[13] Gyorfi, L., Udina, F. and Walk, H. (2008) Nonparametric Nearest Neighbor Based Empirical Portfolio Selection Strategies. *Statistics & Decisions*, **26**, 145-157. https://doi.org/10.1524/stnd.2008.0917

[14] Abbasbandy, S., Roohani Ghehsateh, H., Hashim, I. and Alsaedi, A. (2014) A Com-

parision Study of Meshfree Techniques for Solving the Two-Dimensional Linear Hyperbolic Telegraph Equation. *Engineering Analysis with Boundary Elements*, **47**, 10-20. https://doi.org/10.1016/j.enganabound.2014.04.006

[15] Ji, Y. and Kim, S. (2013) An Adaptive Radial Basis Function Method Using Weighted Improvement. *Winter Simulation Conference Proceeding*, Washington DC, 8-11 December 2013, 957-968. https://doi.org/10.1109/WSC.2013.6721486

[16] Khan, M., Khan, Z. and Khan, H. (2020) Collocation Method for Multiplicative Noise Removal Model. *Mehran University Research Journal of Engineering and Technology*, **39**, 734-743. https://doi.org/10.22581/muet1982.2004.05

[17] Ku, C.Y., Liu, C.Y. and Xiao, J.E. (2020) Multiquadrics without the Shape Parameter for Solving Partial Differential Equations. *Symmetry*, **12**, Article No. 1813. https://doi.org/10.3390/sym12111813

[18] Wang, S.Y. and Wang, M.Y. (2006) Structural Shape and Topology Optimization Using an Implicit Free Boundary Parametrization Method. *Computer Modeling in Engineering & Sciences*, **13**, 119-147.

[19] Tanbay, T. and Ozgener, B. (2014) A Comparison of the Meshless RBF Collocation Method with Finite Element and Boundary Element Methods in Neutron Diffusion Calculation. *Engineering Analysis with Boundary Elements*, **46**, 30-40. https://doi.org/10.1016/j.enganabound.2014.05.005

[20] Soley, F., Barf, M. and Hagh, F. (2018) Inverse Multi-Quadric RBF for Computing the Weights of FD Method: Application to American Options. *Communications in Nonlinear Science and Numerical Simulation*, **64**, 74-88. https://doi.org/10.1016/j.cnsns.2018.04.011

[21] Tan, R., James, R. and Nina, F. (2020) Nonstationary Discrete Convolutionnkenel for Multimodeal Process Monitoring. *IEEE Transaction on Neural Networks and Learning Systems*, **31**, 3670-3681. https://doi.org/10.1109/TNNLS.2019.2945847

[22] Buhmann, D., Marchi, S. and Perra, E. (2020) Analysis of a New Class of Rational RBF Expansions. *IMA Journal of Numerical Analysis*, **40**, 1972-1993. https://doi.org/10.1093/imanum/drz015

[23] Hardy, R.L. (1990) Theory and Application of the Multiquadric-Biharmonic Method 20 Years of Discovery. *Computers and Mathematics with Applications*, **19**, 163-208. https://doi.org/10.1016/0898-1221(90)90272-L

[24] Franke, R. (1982) Scattered Data Interpolation: Tests of Some Methods. *Mathematics of Computation*, **38**, 181-200. https://doi.org/10.1090/S0025-5718-1982-0637296-4

[25] Cover, T.M. (1991) Universal Portfolios. *Mathmatical Finance*, **1**, 1-29. https://doi.org/10.1111/j.1467-9965.1991.tb00002.x

[26] Weiszfeld, E. (1937) Sur le point pour lequel la somme des distance den points donnes est minimum. *Tohoku Mathematical Journal*, **43**, 355-386.

[27] Vard, Y. and Zhang, C.H. (2000) The Multivariate L_1-Median and Associated data Depth. *Proceedings of the National Academy of Science of the United States of America*, **97**, 1423-1426. https://doi.org/10.1073/pnas.97.4.1423

[28] Boyd, J.P. (2011) The Near-Equivalence of Five Species of Spectrally-Accurate Radial Basis Functions (RBFs): Asymptotic Approximations to the RBF Cardinal Functions on a Uniform Unbounded Grid. *Journal of Computational Physics*, **230**, 1304-1318. https://doi.org/10.1016/j.jcp.2010.10.038

[29] Brahma, P., Wu, D.-P. and She, Y.-Y. (2016) Why Deep Learning Works: A Manifold Disentanglement Perspective. *IEEE Transaction on Neural Networks and Learn-*

ing Systems, **27**, 1997-2008. https://doi.org/10.1109/TNNLS.2015.2496947

[30] Jenni, R., Serkan, K. and Mon, G. (2016) Training Radial Basis Function Neural Networks for Classification via Class-Specific Clustering. *IEEE Transaction on Neural Networks and Learning Systems*, **27**, 2458-2471. https://doi.org/10.1109/TNNLS.2015.2497286

[31] John, D., Shai, S.-S. and Yor, S. (2008) Efficient Projections onto the l_1-Ball for Learning in High Dimensions. *International Conference on Machine Learning*, Helsinki, 5-9 July 2008, 272-279.

[32] Lai, Z.-R., Yang, P.-Y., Wu, X.-T. and Fang, L. (2018) Trend Representation Based Log-Density Regularization System for Portfolio Optimization. *Pattern Recognition*, **76**, 14-24. https://doi.org/10.1016/j.patcog.2017.10.024

[33] Lai, Z.-R., Yang, P.-Y., Fang, L.-D. and Wu, X.-T. (2018) Short-Term Sparse Portfolio Optimization Based on Alternating Direction Method of Multipliers. *Journal of Machine Learning Research*, **19**, 63:1-63:28.

[34] Lai, Z.-R., Dai, D.-Q., Ren, C.-X. and Huang, K.-K. (2018) Radial Basis Functions with Adaptive Input and Composite Trend Representation for PS. *IEEE Transaction on Neural Networks and Learning Systems*, **29**, 6214-6226. https://doi.org/10.1109/TNNLS.2018.2827952

[35] Jegadeesh, N. (1990) Evidence of Predictable Behavior of Security Returns. *The Journal of Finance*, **45**, 881-898. https://doi.org/10.1111/j.1540-6261.1990.tb05110.x

[36] Sharpe, W.F. (1964) Capital Asset Prices: A Theory of Market Equilibrium under Conditions of Risk. *The Journal of Finance*, **19**, 425-442. https://doi.org/10.1111/j.1540-6261.1964.tb02865.x

[37] Lintner, J. (1965) The Valuation of Risk Assets and the Selection of Risky Investments in Stock Portfolios and Capital Budgets. *The Review of Economics and Statistics*, **47**, 13-37. https://doi.org/10.2307/1924119

[38] Mossin, J. (1966) Equilibrium in a Capital Asset Market. *The Econometric Society*, **34**, 768-783. https://doi.org/10.2307/1910098

[39] Sharpe, W.F. (1966) Mutual Fund Performance. *The Journal of Business*, **39**, 119-138. https://doi.org/10.1086/294846

[40] Treynor, J.L. and Black, F. (1973) How to Use Security Analysis to Improve Portfolio Selection. *The Journal of Business*, **46**, 66-86. https://doi.org/10.1086/295508

[41] Blum, A. and Kalai, A. (1999) Univeral Portfolios with and without Transaction Costs. *Machine Learning*, **35**, 193-205. https://doi.org/10.1023/A:1007530728748

[42] Aldrige, I. (2013) High-Frequency Trading: A Practical Guide to Algorithmic Strategies and Trading Systems. 2nd Edition, Wiley, Hoboken. https://doi.org/10.1002/9781119203803